

# A NOVEL APPROACH TO FINGER VEIN AUTHENTICATION

Fotios Tagkalakis<sup>†</sup>, Dimitrios Vlachakis<sup>\*</sup>, Vasileios Megalooikonomou<sup>\*</sup>, Athanassios Skodras<sup>†</sup>

<sup>†</sup> Department of Electrical and Computer Engineering, University of Patras, Patras, Greece

<sup>\*</sup> Computer Engineering and Informatics Department, University of Patras, Patras, Greece  
ece7931@upnet.gr, {vlachakis, vasilis}@ceid.upatras.gr, skodras@upatras.gr

## ABSTRACT

Finger vein patterns are unique biometric features, which differentiate from individual to individual, so they are suitable for authentication applications. Systems based on the use of this feature have numerous advantages such as low cost and high accuracy. A new finger vein authentication approach is proposed, which is based on the efficient detection of the non-vein regions, in order to define the main vein patterns. The proposed method is robust in extracting and depicting not only the finger's vein pattern, but also other important features such as the veins' width. The authentication algorithm has been evaluated on a finger vein database of 400 images. The false acceptance and false rejection rates achieved are 0% and 0.5% respectively.

**Index Terms**— biometrics, finger vein authentication, bio-identity, digital signatures, person identification

## 1. INTRODUCTION

Biometric authentication refers to the retrieval of a person's identity based on physical traits. Numerous biometric characteristics are being used for authentication, such as fingerprints, voice, face, palm, finger veins, or even iris. The most commonly used biometric modalities are the fingerprints and the face images. Soft biometrics are also employed, i.e. behavioral or adhered human characteristics, such as gait or keystroke. Each of the above possesses has its own advantages and disadvantages with regards to accuracy, security, cost and ease of use. Table 1 summarizes the main biometric modalities and their properties<sup>[1]</sup>.

Finger vein images, captured at the near-infrared (NIR) spectrum, is an emerging authentication method as it presents a lot of advantages: low forgery risk, detection of person's aliveness, non-invasive data acquisition. The hemoglobin of the blood absorbs the infrared light, making the veins visible as darker areas inside the finger<sup>[2]</sup>. The applications of the finger vein authentication cover the fields of the public sector, logistics, healthcare, welfare, education and finance<sup>[3]</sup>. Finger vein authentication systems are already installed in more than hundred cities in Japan

Table 1: Authentication systems based on different modalities

	Voice	Iris	Fingerprints	Face	Veins
Accurate		✓	✓		✓
Secure		✓			✓
Easy to use	✓		✓	✓	✓
Low cost	✓		✓	✓	✓

and in other countries worldwide mainly for banking services (Automatic Teller Machines).

During the last years, numerous methods have been proposed for person identification via the finger veins' patterns. Some of the most interesting works are those of Gongping Yang et. al.<sup>[4]</sup>, Bakhtiar Affendi Rosdi et. al.<sup>[5]</sup> and Naoto Miura<sup>[6]</sup>.

In this paper a new approach for the improvement of the performance of a finger vein authentication system is proposed. In the proposed method, the NIR finger vein images are processed in a way that the non-vein areas are greatly enhanced, resulting in better feature extraction and eventually improved pattern matching.

## 2. PROPOSED APPROACH

The flowchart of the proposed approach is depicted in Fig.1. The captured NIR finger vein image undergoes a pre-processing in order for its brightness to be enhanced and thus facilitate non-vein detection during the following stages. Based on the findings of this stage, the vein pattern is extracted and improved pattern matching is achieved facilitating the authentication. The detailed description of each stage is given below.

### 2.1. Stage 1: Preprocessing

In the preprocessing stage several characteristics of the image are modified so that useful information is exploited. One of the first problems that has to be resolved is the fact that the images consist of unwanted areas, which needed to be removed. In order to achieve this, the images are cropped so that information is taken mostly from the finger region. *Image enhancement* and *contrast enhancement* constitute the rest of the pre-processing procedure.

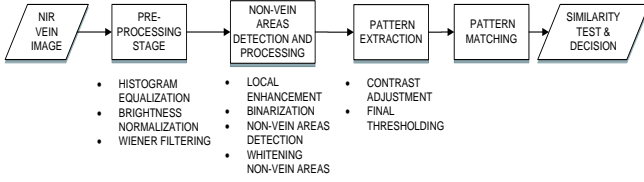


Figure 1: Flowchart of the proposed method

Image enhancement begins with histogram equalization. More specifically, the histogram of the near infrared image originally captured is redistributed so that a uniform population density is produced in order to secure that certain adjacent gray values are grouped. Any peaks and valleys contained in the histogram of the original image are maintained, although they are shifted. In histogram equalization each pixel is assigned a new intensity value based on its original one. Given  $L$  is the number of possible intensity values,  $p$  is the normalized histogram of image  $f$  and  $g$  is the histogram-equalized image:

$$p_l = \frac{\text{\#of pixels with intensity } l}{\text{total \#of pixels}} \quad (1)$$

where  $l=0,1,2, \dots, L-1$  and

$$g(i, j) = \text{floor}((L-1) \sum_{l=0}^{f(i,j)} p_l) \quad (2)$$

The enhancement of the image's contrast is performed by transforming the values of the grayscale image using contrast-limited adaptive histogram equalization (CLAHE). This process normalizes the brightness of the image by operating on small regions of the image (image *tiles*), rather than the entire image. Each tile's contrast is enhanced, so that the histogram of the output region approximately matches a histogram specified a priori. In our case a histogram consists of 500 bins, following an exponential distribution, with contrast enhancement limit equal to 0.07. The neighboring tiles are then combined using bilinear interpolation.

The image enhancement sub stage is completed by applying a two-dimensional adaptive noise removal Wiener filter. It is assumed that the grayscale image is degraded by constant power additive noise. More specifically a pixel wise adaptive Wiener method is used, which is based on statistics estimated from a local neighborhood of each pixel.

## 2.2. Stage 2: Non-vein areas detection and processing

A local contrast enhancement procedure takes place using the histogram statistics<sup>[7]</sup>. In detail, a 3x3 square neighborhood is defined and the center of this area is moved from pixel to pixel along the image in raster order. Mean and standard deviation are known statistical measures, which in this case are used for enhancement purposes.

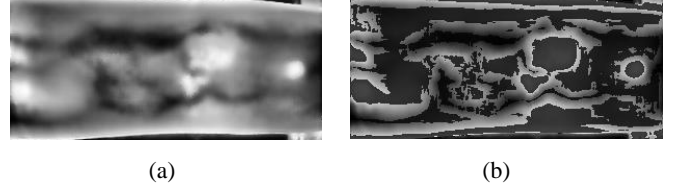


Figure 2: (a) Stage 1 output and (b) same image after local contrast enhancement

Initially, they are measured over the entire image. After that, the same measurements are conducted for the neighborhood at hand. Then, the local mean and standard deviation are compared with fractions of their respective global values. Specifically, it is checked if local mean deviation is less than 1.5 times its global value and local standard deviation's value is between 0.75 and 1.5 times its respective global value. In case the above mentioned criteria are met, the value of the center pixel of the neighborhood is increased. The center of the neighborhood region is then moved to an adjacent pixel location and the procedure is repeated.

Examining the output image of the local contrast enhancement procedure, which is depicted in Fig.2, an important observation can be made: the brighter pixels mark the area surrounding the veins. Moving to the next stage of the proposed algorithm non-vein areas are detected and processed. Initially, the contrast enhanced image is binarized. Otsu's method<sup>[8]</sup> is used in order to indicate a suitable threshold value (given an original image  $a$ ), new values are assigned to each pixel creating a new image  $b$ .

Next, the non-vein areas' boundaries are detected. Specifically, the sets of points, which constitute the contour of these areas, are calculated. In order to achieve this, the binary image  $b$  is examined and the connected components of it, are detected and assigned a level to the pixels that constitute each component.

The exact coordinates of the non-vein areas' contours are used in order to force these specific areas, to have an externally imposed far higher contrast than the one they already had, in comparison to their adjacent areas. To do so all the pixels included in these non-vein areas have their values changed to 255. This change of values is now performed to the image taken as output of *Stage 1*, as in this image the vein areas are depicted clearer than in any other.

The output of *Stage 2* is shown in image (a) of Fig.3. This image shows the whitened non-vein areas of the finger's image; these will be used as input for the next stage of the algorithm.

## 2.3. Stage 3: Pattern extraction

During this stage, the pattern extraction procedure takes place. At the beginning of this stage the finger image with the whitened non-vein areas has its contrast adjusted (the intensity values in grayscale image are mapped to new values such that 1% of data is saturated at low and high intensities of the original grayscale image). After that a final



Figure 3: (a) Stage 2 output and (b) the extracted pattern

thresholding is required for the pattern extraction to be completed. The threshold used at this point is the same one with that calculated before (the outcome of the Otsu's Method for the local contrast enhanced image).

Moreover, the finger's envelope is detected by applying a simple horizontal line detection filter  $[-1, -1, -1; 2, 2, 2; -1, -1, -1]$  and then subtracted from the patterns. The morphological operation of closing, with a structuring element of disk shape with a radius of 9 pixels, is then applied on the patterns, in order to remove any remaining noise and bridge some of the gaps existing in the pattern. All the above mentioned procedures reassure the fact that the algorithm detects most of the parts of the main veins included in the finger. An example of such a vein pattern extraction is shown in Fig.3 (b).

It is important to mention that experiments indicated that if (the very same) above mentioned algorithmic steps (*Stages 1-3*) are applied to blocks of the NIR image instead of the whole image, better exploitable patterns are produced. More specifically, the initial NIR images, are partitioned in six sub-images (of the same size); each one of them is used successively as input for the algorithm producing its own pattern. The six sub-patterns produced by the algorithm are suitably merged into one image producing the optimal pattern. The NIR image divided in six sub-images and the optimal pattern produced by them are shown in Fig.4. In agreement with this concept the optimal patterns are used as basis for the next stage.

#### 2.4. Stage 4: Pattern matching

In the pattern matching stage the optimal vein patterns produced in the previous stages are used in order to conduct the needed comparisons. A single criterion is enough to achieve satisfying error percentages. Let's assume that  $f$  is the vein pattern produced by the processing of the original image and  $w$  is the vein pattern produced by the processing of the query image. Firstly, FFT is used to convert  $f$ ,  $w$  from time domain to frequency domain as  $F$ ,  $W$  respectively. Secondly, the complex conjugate of  $W$  is calculated and denoted as  $W^*$ . Afterwards,  $F$  is multiplied by  $W^*$  and their product is converted to time domain by the IFFT. The process described above is the calculation of the correlation in the frequency domain<sup>[9]</sup>. The outcome of this process is an image  $r$ . The maximum value of  $r$  indicates the maximum number of matched pixels of the two images  $f$  and  $w$ . In order to check if the two patterns are matched, two

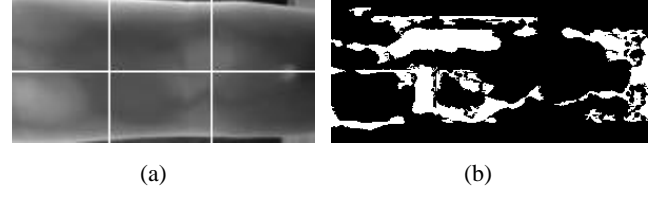


Figure 4: (a) NIR image divided in 6 equal sub-images and (b) the optimal pattern

ratios  $S_r$  (similarity ratio) and  $D_r$  (difference ratio) are used, defined as follows:

$$S_r = \frac{\max(r)}{N} 100\% \quad (3) \quad D_r = \frac{|N - N_q|}{N} 100\% \quad (4)$$

where  $N$  is the number of white pixels in the original image and  $N_q$  is the number of white pixels in the query image. If:  $S_r > 60.5\%$  and at the same time  $D_r < 23.8\%$  the two compared images are considered to match. The threshold value for the  $S_r$  is the second smaller  $S_r$  value found by the comparison of every possible couple of images depicting the same person's finger. Respectively, the  $D_r$  threshold is the largest  $D_r$  percentage found by the same comparison.

### 3. EXPERIMENTAL RESULTS

During the experimental procedure a test base was created by randomly selecting images out of a publically available finger vein database<sup>[10]</sup>. This particular finger vein database was also used in previous work<sup>[11]</sup>. The final test base consists of 200 folders, each one of them consisting of two different images of an individual's finger. Each image is grayscale of size  $320 \times 240$  pixels. 40.000 different comparisons were conducted. In detail, the first 200 comparisons were between the two images included in each of the 200 files. The rest 39.800 of them, were between images from different folders, i.e. from different individuals' fingers.

The results obtained from the comparisons, are the following: one out of the two hundred comparisons faulty rejected a query image, while no images were faulty accepted out of the 39.800 comparisons. Therefore, the percentages calculated are: FRR (false rejection rate)=0.5% and FAR (false acceptance rate) =0%.

### 4. DISCUSSION

It is important to underline that according to the results, the proposed algorithm is considered to be a highly secure and accurate choice when it comes to person identification. First of all the use of the finger vein patterns itself, does not permit conventional attempts of forgery. On top of that the zero percentage of the FAR indicates that the system would not be easily deceived by an individual's (query) finger image, which is even slightly different from the original.

Table 2: Comparative summary of relative work

Reference	Methodology	Database (# users)	Performance
Rosdi, Shing <sup>[5]</sup>	Local Line Binary Pattern	51	FAR=1.78% FRR=1.78%
Tang, Huang <sup>[12]</sup>	Tracing, Extracting and Encoding finger vein patterns	1200	FAR=1.5% FRR=1.5%
Shareef et al <sup>[13]</sup>	Haar Wavelet Transform	106	FAR=0.2% FRR=0.2%
Tagkalakis et al <sup>[11]</sup>	Maximum Curvature	106	FAR=0% FRR=1.00%
Proposed	Non-vein Region Detection	106	FAR=0 % FRR=0.5%

As for the FRR percentage of 0.5%, it originates from the fact that in the 200 comparisons which were supposed to accept the given query image, one image was faulty rejected. This rejection is caused probably by the fact that the finger was either bent or twisted in a way that some details differentiated the two images. Such placement issues could be avoided if the capturing device did not allow for the finger to be misplaced.

The results of the proposed method are indeed satisfying, as they appear to have smaller error rates than other conventional methods as shown in Table 2. For example, the Local Line Binary Patterns<sup>[5]</sup> provides equal values for FAR and FRR (1.78%). Another approach is proposed in<sup>[12]</sup>, where FAR=FRR=1.5%. Both of the above mentioned error rates seem to exceed by far those of the proposed approach. Perhaps, the most important comparisons can be done between the proposed approach and that of<sup>[13]</sup>, as both are based on the same database.

In Asmaa Q. Shareef's et al work<sup>[13]</sup> the exact number of the comparisons is not stated, but assuming that it is close to the number of comparisons conducted in this study, the error rates presented can be well compared. The proposed approach seems to have a FRR higher by 0.3% compared to<sup>[13]</sup>, but it has to be underlined that this percentage was calculated by 200 comparisons. As for the FAR, which is by far the most crucial error rate, the proposed algorithm achieves 0% which is based on the solid ground of the 39.800 comparisons conducted between different individuals' fingers. It is straightforward to conclude that the presented algorithm prevails over the above mentioned one, as in the worst case scenario it would force the user to take a second shot of his finger (faulty rejectance), while it is reassured that a person's identity would never be misinterpreted.

Finally, comparing this study with previous works<sup>[11]</sup> in which the same images were used as test-base, the FRR is now half as large and the FAR has kept its zero percentage.

## 5. COCLUSIONS

The need to achieve personal identification in a secure, robust and low cost way is a clear demand in nowadays. As

this study shows, the proposed algorithm is in position to be used in a vast variety of technologically advanced applications such as internet banking, physical access control systems and even digital issuing of certificates. In addition, the extracted vein patterns can be considered useful biomedical images as they contain information for significant features such as vein width, number and type of bifurcations etc. For example, vein extraction is used in vascular pathology improving diagnosis and follow up of angiogenesis in human body<sup>[14]</sup>.

## 6. REFERENCES

- [1] Eliza Strickland, "Blood and Money", IEEE Spectrum, Vol. 49, No. 6, pp. 33-37, June 2012.
- [2] Zharov VP, Ferguson S, Eidt JF, Howard PC, Fink LM, Waner M. Infrared Imaging of Subcutaneous Veins. *Laser Surg Med* 2004; 34: 2004.
- [3] Yuri Nakamaru, Makiko Oshina, Suichi Murakani, Ben Edgington, Ravi Ahluwalia, "Trends in Finger Vein Authentication and Deployment in Europe", *Hitachi Review*, Vol. 64, No. 5, pp. 275-279, 2015.
- [4] Gongping Yang, Xiaoming Xi, Yilong Yin, "Finger Vein Recognition Based on a Personalized Best Bit Map", in *Sensors* 2012, 12(2), 1738-1757.
- [5] Bakhtiar Affendi Rosdi, Chai Wuh Shing, Shahrel Azmin Suandi, "Finger Vein Recognition Using Local Line Binary Pattern", in *Sensors* 2011, 11(12), 11357-11371.
- [6] Naoto Miura, Agio Nagasaka and Takafumi Miyatake "Extraction of Finger-Vein Patterns Using Maximum Curvature Points in Image Profiles", in MVA2005 IAPR Conference on Machine Vision Applications, May 16-18, Tsukuba Science City, Japan, 2005.
- [7] Cristian Ordoyo Casado, "Image Contrast Enhancement Methods", in Technical University - Sofia (Faculty of telecommunications) in <http://academica-e.unavarra.es/xmlui/bitstream/handle/2454/2368/577327.pdf?sequence=1&isAllowed=y>
- [8] Nobuyuki Otsu (1979). "A Threshold Selection Method from Gray-Level Histograms". *IEEE Trans. Sys., Man., Cyber.* 9 (1): 62-66.
- [9] Trung Huynh, "Finger Vein Authentication System", in University of Plymouth, in [http://www.academia.edu/179273/Finger\\_Vein\\_Authentication\\_System\\_Report](http://www.academia.edu/179273/Finger_Vein_Authentication_System_Report) [accessed March 2015].
- [10] Finger vein database by Wuhan University, in <http://mla.sdu.edu.cn/sdumla-hmt.html> [accessed March 2015].
- [11] Fotios Tagkalakis, Vassilis Fotopoulos, "A Low Cost Finger Vein Authentication System, using Maximum Curvature Points", in *Applied Electronics (AE)*, International Conference 8-9, pp. 249-252, Sep. 2015.
- [12] Darun Tang, Beining Huang, Rongfeng Li, Wenxin Li, "A Person Retrieval Solution Using Finger Vein Patterns", in *ICPR Proceedings of the 20th International Conference on Pattern Recognition*, pp. 1306-1309, 2010.
- [13] Asmaa Q Sharref, Loay E. George, Roaa E Fadel, "Computing Finger Vein Recognition Using Haar Wavelet Transform", in *International Journal of Computer Science and Mobile Computing*, 4(3), pp. 1-7, March 2015.
- [14] Marios Vlachos, Evangelos Dermatas, "Vein Segmentation in Infrared Images Using Compound Enhancing and Crisp Clustering", in *Computer Vision Systems: 6<sup>th</sup> International Conference on Computer Vision Systems*, Santorini, Greece, pp.393-401, 2008.